SUPPLEMENTAL DATA

Table S1. Primers used in this study.

Number	Sequence	Restriction Enzyme
A115	GGTCAGACCAGTTCGGGGGTCAC	
A118	GTGGTCATGGGGATGCGGACTTC	
A193	TGGAACTGGCCGATGCGT	
A194	TCAAGTCACTGCCGGGGTT	
A197	ACGTCGGCACTACCCGTCT	
A198	ACGCGCCCGATCACATAG	
A215	GAAGGAATTACATATGGGCAACAATGTCCCG	NdeI
A216	GCTAGAGTACTTGTCTTCCTGAACCCCGC	ScaI
A217	TTTTTTTTCCAAAGAATGGATCTACGTCGTCACCGAAGC	Van91I
A218	TTTTTTTTCCAACGCATGGGAACCCGACCACCAGTCTG	Van91I
A219	TTTTTTTTCCATGCGTTGGGGAGTAACCATCGACCTGGC	Van91I
A220	TTTTTTTTCCAACTTTTGGCGAGCTGACACCGGAGAC	Van91I
A470	AAAGGTACCAAGTCCTCCCGGCTCGT	KpnI
A472	TTTTTTCTAGAGCTTAGCCCGCGTAGTCCGGGACGTCGTACGGGT AAGCTCTTCCTGTCTTCCTGAACCCCGC	XbaI-BlpI-HA-BspQI
A522	CACCGTGACCGATTTCGGAGCAGCC	
A523	TCATGTCTTCCTGAACCCCGCCAGGTC	

Restriction enzyme sites are underlined.

Table S2. Colony size of suppressor mutants, S4 and S21, after transformation of LmeA-HA expression vector.

Strain	Colony Size (mm)
WT	3.17 ± 0.69
S4 + LmeA	2.79 ± 0.64
S21 + LmeA	3.84 ± 0.96

The data shown are average ± standard deviation. N = 10.

Supplemental Figure Legends

Figure S1. Profiles of PIMs purified from suppressor mutants analyzed by TLC and visualized by orcinol staining. None of the suppressor mutants show AcPIM6 production. Only a part of TLC plates is shown.

Figure S2. Characterization of LM and LAM in the suppressor mutants. LM/LAM were separated by SDS-PAGE and visualized by ProQ Emerald glycan staining. Black arrows indicate the accumulation of smaller LM or LAM.

Figure S3. Markerless deletion of *lmeA*. A) The genomic region covering the upstream and downstream of *lmeA*. Upper panel, WT; lower panel, Δ*lmeA*. Arrows and boxes A217, A218, A219, and A220 indicates the primers used to create the knockout construct, pMUM57. Grey arrows and boxes, forward primers; green arrows and boxes, reverse primers. B) The confirmation of *lmeA* deletion by PCR using A217 and A220. Expected sizes were 3.29 kbp (open arrowhead) for WT or 2.50 kbp (filled arrowhead) for Δ*lmeA* (DXO). In the single crossover (SXO) strain, both bands are expected.

Figure S4. Analysis of Δ*lmeA*. A) Markerless deletion of *lmeA* does not impact other phospholipids. Crude lipid extracts of WT and Δ*lmeA* were separated on TLC and stained with iodine. CL, cardiolipin. B) LmeA-HA carrying missense mutations found in the suppressor mutants S1 and S10 cannot rescue the Δ*lmeA* phenotype. Δ*lmeA* was transformed with an expression vector for LmeA G170D or V181G mutant. ProQ Emerald staining of LM/LAM separated by SDS-PAGE. C) Western blot showing that LmeA-HA carrying the G170D or V181G point mutation was not detected. Ponceau S staining shows protein loading in each lane.

Figure S5. LmeA is conserved in the *Corynebacteriales* order. A) A protein phylogeny of LmeA and its orthologs. Orthologs were identified throughout the *Corynebacteriales* order. A., *Amycolicicoccus*; C., *Corynebacterium*; D., *Dietzia*; G., *Gordonia*; M., *Mycobacterium*; N., *Nocardia*; R., *Rhodococcus*; S., *Segniliparus*; T., *Tsukamurella*. The phylogenic tree was created using Geneious 10.1 (Biomatters) with the following settings: cost matrix, identity; genetic distance model, Jukes-Cantor; method, neighbor joining. Branch length indicates amino acid substitutions per site. B) Homology alignment of *Msmeg* LmeA, MSMEG_5785, and *Mtb* LmeA, Rv0817c, showing several highly conserved regions (shaded in black) and overall 60% identity. The missense mutations found in the suppressor mutants S1 and S10 are marked by * and #, respectively.

Figure S6. Dose response of LmeA binding to various lipids. A) Cupric acetate staining of 0.7 nmol of PE and TAG developed with hexane / diethyl ether / formic acid (40:10:1). B-C) Cupric acetate staining of 0.7 nmol of PI and PE (panel B) or PE, PA, and GGP (panel C) developed with chloroform / methanol / 13 M ammonia / 1 M ammonium acetate / water (180:140:9:9:23). D-I) Dose response of His-LmeA to LM intermediates, PE, PI, PA, TAG, or GGP. T, lysate of *E. coli* cell transformed with the His-LmeA expression vector; UT, lysate of untransformed *E. coli*. Both lysates were prepared after 3 hour IPTG induction. Note that the concentration range of GGP is different from those of the other lipids.

Figure S7. Soluble mannose-containing molecules do not competitively inhibit the binding of LmeA to PE. No competitor (None), 10 mM mannose 1-phosphate (M1P), or 10 mM GDP-Man was pre-incubated with *E. coli* cell lysate expressing LmeA before addition of lysate to the microtiter plate coated with 1.25 μM PE.

Supplemental Figure 1

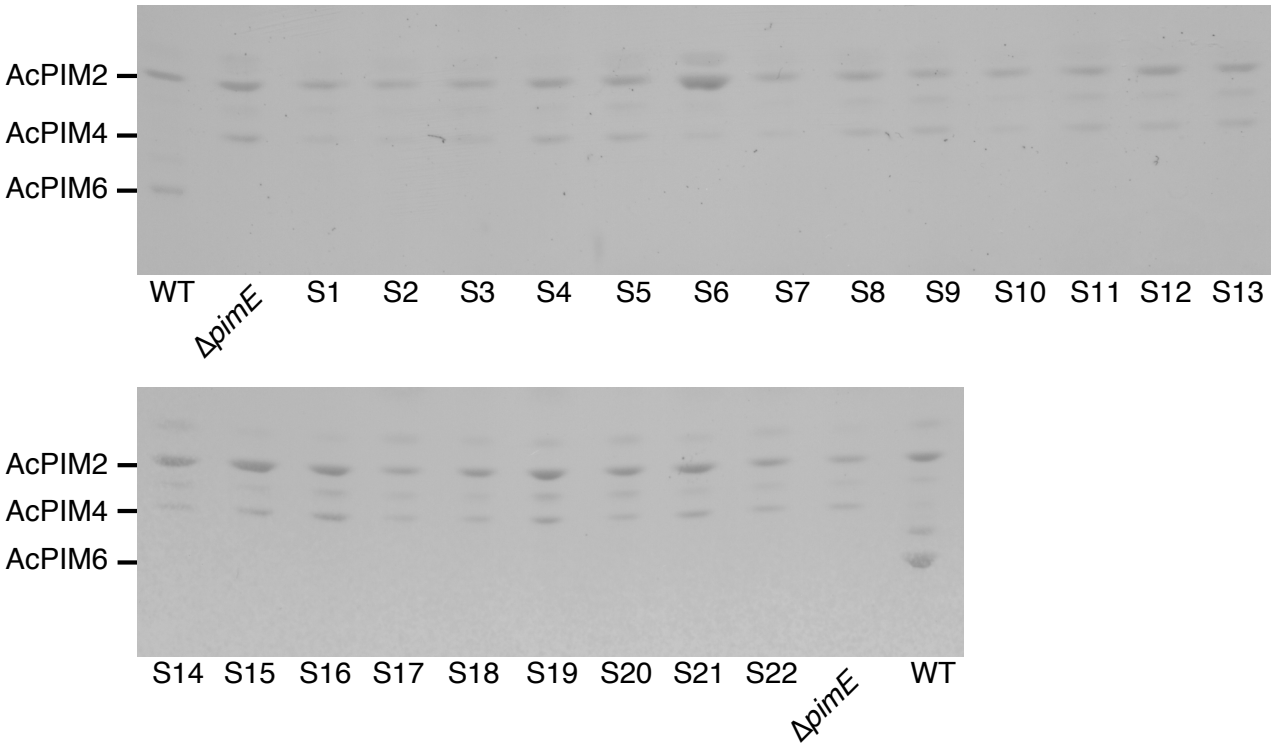

Supplemental Figure 2

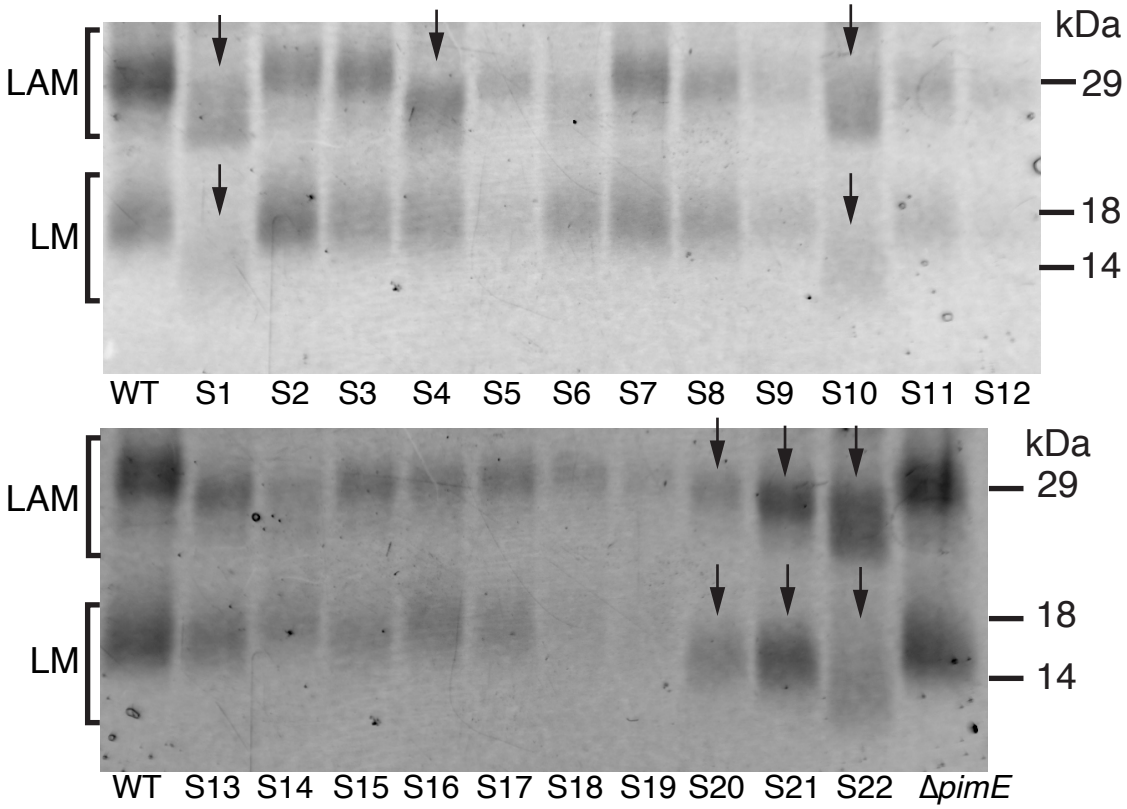

Supplemental Figure 3

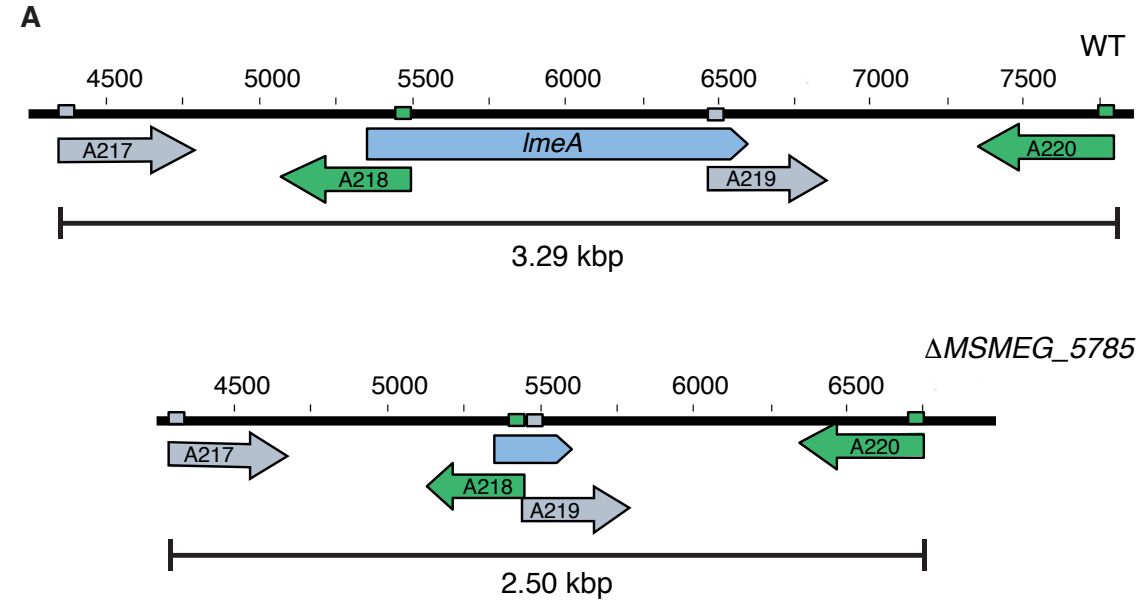

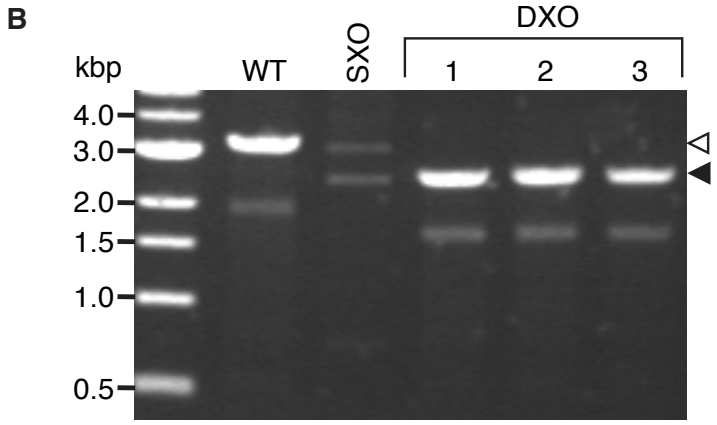

Supplemental Figure 4

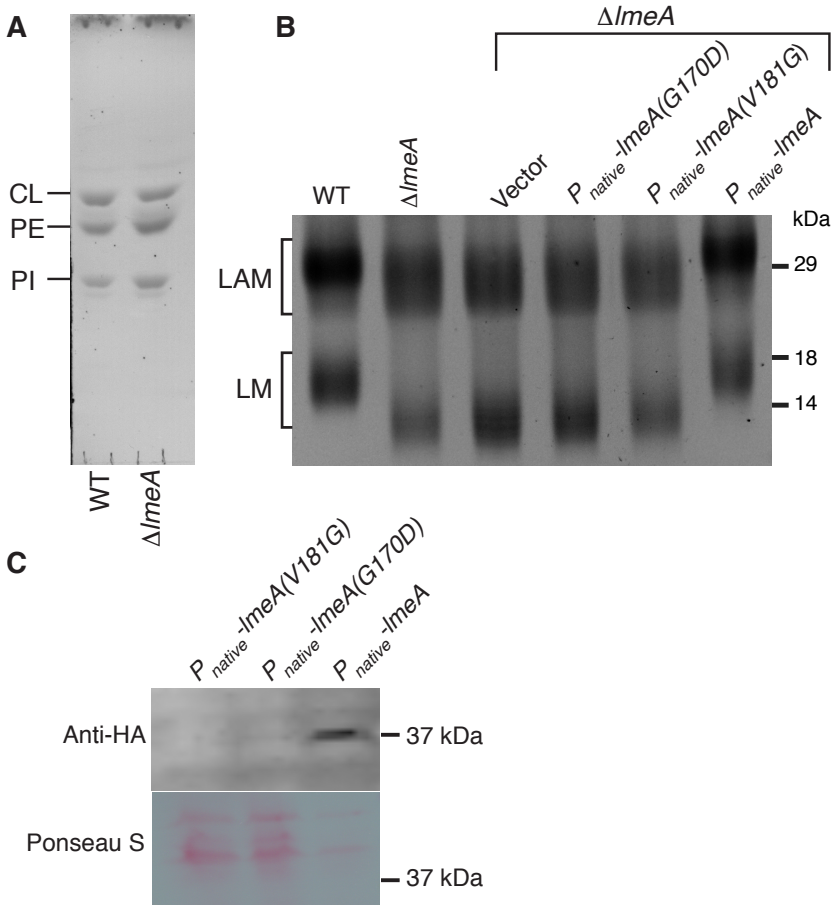

Supplemental Figure 5

A

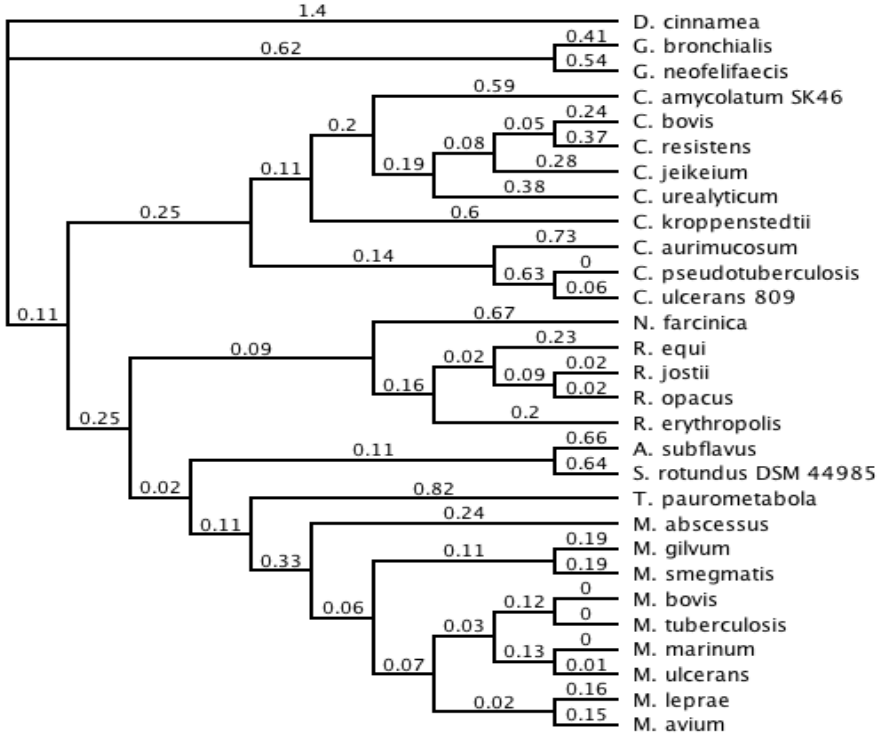

B

```
M.tuberculosis     1 MPMRKVLVGVTGAAIVVAVLIVGAVGA-DFGASIYAEYRLSTTVRKAANLRSDPFVAILR
M.smegmatis        1 MGNNVPVRRLVVGFVAAVAALVVGAVGTDFGAAIYAEYRLARTVRSAASLNWDPWVAILG

M.tuberculosis    60 FPFIPQAMREHYAELEIKAFAVEHAGSGTATLEATMHSIDLSYASWLIRPDAKLPVGELP
M.smegmatis       61 FPFIPQARDHRYNEIEIRANGVDHPVAEKVSLEATLHDVDITEASWLIREDAPLPVAEAE

M.tuberculosis   120 SRIIIDSMHLGRYLGISDLMVAAPRQESNDATGGTTESGISGSRGLVFSGTPISANFAHR
M.smegmatis      121 SRIIIDSTHVGRYMGIDDLLVEAPSRDTNDATGGTTESGISGNTGLVFTGTPKASGLDKR

                     #
M.tuberculosis   180 VSVLVDLSVASDDRATLVITPTAVVTGPDTADQPVPDDKRDAVLHAFASKLPNQKLPFGV
M.smegmatis      181 VSVAVDLSLEGPDQSTLVLTATGILTGPNTADEQVPDDKLASVLDEFSNTIPDLRLPFGI

M.tuberculosis   240 VPNTVGARGSDVIIEGITRGVTISLDEFKQS
M.smegmatis      241 APTSQGARGSDIIIEGIGEGVTIDLAGFRKT
```

Supplemental Figure 6

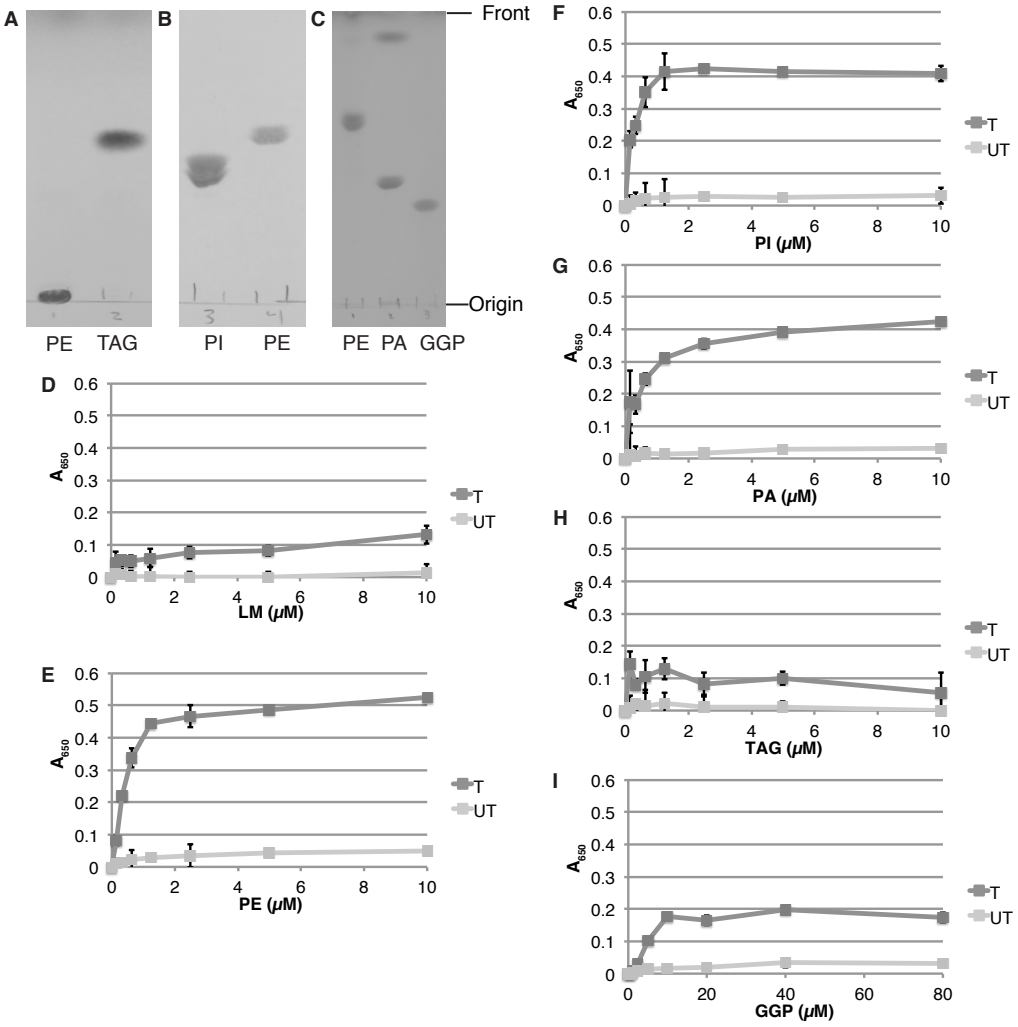

Supplemental Figure 7